Astron. Astrophys. 336, L49–L52 (1998)

ASTRONOMY AND ASTROPHYSICS

LETTER

Letter to the Editor

First statistical data on wavefront outer scale at La Silla observatory from the GSM instrument

F. Martin[1], **A. Tokovinin**[2], **A. Ziad**[1], **R. Conan**[1], **J. Borgnino**[1], **R. Avila**[1], **A. Agabi**[1], **and M. Sarazin**[3]

[1] U.M.R. Astrophysique N^o 6525 - C.N.R.S. - Université de Nice-Sophia Antipolis, F-06108 Nice Cedex 2, France
[2] Sternberg Astronomical Institute, Universitetsky prosp., 13, 119899 Moscow, Russia
[3] European Southern Observatory, Karl-Schwarzschild-Strasse 2, D-85748 Garching bei München, Germany

Received 9 March 1998 / Accepted 8 July 1998

Abstract. Results of the first monitoring of the wavefront outer scale $\mathcal{L}_0$ during 16 nights at La Silla, Chile, are presented. This parameter is of importance for high angular resolution observing techniques like adaptive optics and optical interferometry. It was measured with the Grating Scale Monitor (GSM) instrument which is based on the analysis of the spatial covariance of angle of arrival fluctuations simultaneously detected at several points on the wavefront. The outer scale distribution is found to be log-normal, with median value of 24 m and rms scatter of $\log\mathcal{L}_0$ of ± 0.22. Short-duration bursts of $\mathcal{L}_0$ are noted. During 1 hour the $\mathcal{L}_0$ and seeing were simultaneously measured with the ADONIS adaptive optics system at the 3.6 m telescope, and a good agreement with our data was noted.

Our measurements of the seeing were found to agree with the ESO DIMM seeing data. Effective wavefront velocity was also found in order to estimate the adaptive optics time constant.

Key words: seeing – adaptive optics – interferometry

Fig. 1. View of the GSM instrument at La Silla. The central pier with two modules in differential configuration is seen on the left, the eastern module in the center and the southern module on the right.

1. Introduction

Substantial progress in astronomical imagery has been recently achieved due to the rapid development of high angular resolution (HAR) techniques like adaptive optics (AO) and long baseline optical interferometry (LBI). It is known that these techniques are severely influenced by atmospheric turbulence (Roddier 1981). To quantify atmospheric effects, it is necessary to know several parameters directly related to the wavefront structure, namely Fried's parameter r_0 which defines the FWHM seeing angle $\beta = 0.98\lambda/r_0$, the characteristic time constant, the isoplanatic angle and the wavefront outer scale $\mathcal{L}_0$. $\mathcal{L}_0$ is an optical parameter integrating atmospheric turbulence effects along the whole propagation path (Borgnino 1990). Its influence on spatial and temporal statistics of the wavefront becomes significant when values of $\mathcal{L}_0$ are of the order of the telescope aperture or the interferometer baselines (Winker 1991; Voitsekhovitch & Cuevas 1995). $\mathcal{L}_0$ defines the maximum size of wavefront perturbations and is poorly known: values ranging from 2 m to 2000 m were published (Avila et al. 1997). Here we present the first large and homogeneous data set on $\mathcal{L}_0$ which permits the evaluation of the statistical behaviour of the outer scale at a major astronomical site.

Send offprint requests to: F. Martin

2. The GSM instrument: principle

The Grating Scale Monitor (GSM) can be considered as a Shack-Hartmann kind of technique based on measurements of angle of arrival (AA) fluctuations at several points on the wavefront. A statistical analysis of the recorded AA is performed to estimate spatial and temporal wavefront parameters. The prototype version of the instrument is described by Martin et al. (1994), and the first $\mathcal{L}_0$ measurements were published by Agabi et al. (1995).

The instrument consists of four 10-cm telescopes on equatorial mounts (Fig. 1). Each telescope is equipped with a detection module which is capable of measuring synchronously

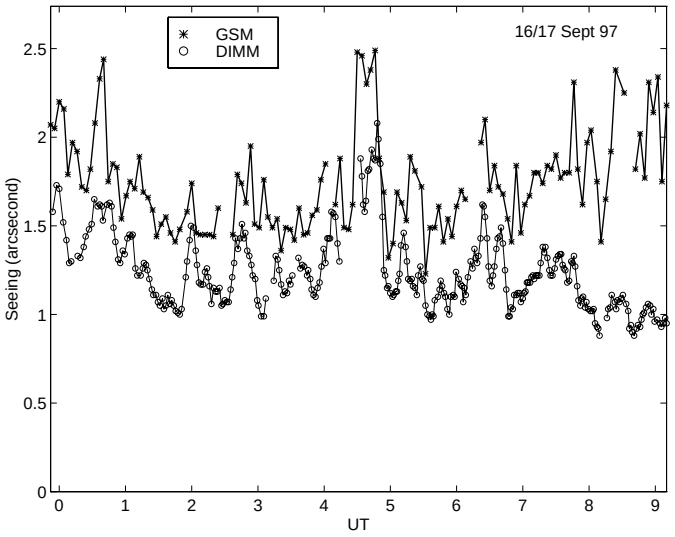

Fig. 2. Comparison of simultaneous seeing measured by ESO DIMM and by GSM

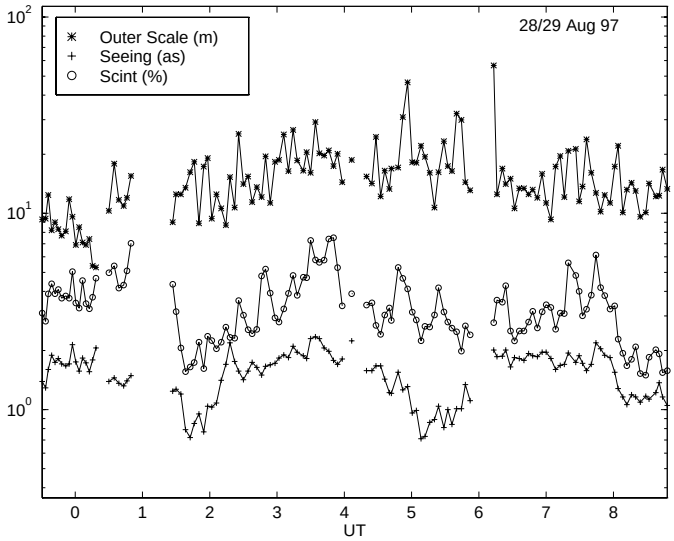

Fig. 3. Temporal evolution of $\mathcal{L}_0$, scintillation index and seeing (upper, middle and lower curves, respectively) during the night of August 28/29. Arrows indicate $\mathcal{L}_0$ bursts.

the AA in the declination direction with a 5 ms sampling time. Two telescopes are installed on a common mount on the central pier and work as a differential image motion monitor (DIMM) (Sarazin & Roddier 1990) with a 25 cm baseline measuring r_0. Two other telescopes have separate mounts on separate piers, located 0.8 m to the south and 1 m to the east from the central pier, thus forming an L-shaped configuration. Telescope objectives were situated 1.5 m above the ground.

A typical measurement sequence consists of 2 mn data acquisitions repeated continuously every 4 mn. Pairwise telescope combinations provide 6 baselines ranging from 25 cm to 1.28 m. The AA covariances are computed for each baseline and normalized by the differential variance of the AA on the 25-cm baseline. They are compared to theoretical normalized covariances and the appropriate $\mathcal{L}_0$ is found for each baseline. Before comparison, the baselines (length and orientation) are projected on to the wavefront plane. The final value of $\mathcal{L}_0$ is taken as a median of individual $\mathcal{L}_0$ values and its error is estimated from their scatter.

Theoretical normalized covariances are computed in the framework of the Von Kàrmàn model (Avila et al. 1997, Eq. 7) in which $\mathcal{L}_0$ appears in the phase power spectrum as the inverse of a spatial frequency. Our study has shown that theoretical normalized covariances are most sensitive to $\mathcal{L}_0$ at baselines less than $\mathcal{L}_0/10$ which explains our choice of baselines of the order of a meter. The $\mathcal{L}_0$ measured by the GSM can be viewed as a parameter of the Von Kàrmàn turbulence model which provides an adequate description of the wavefront structure at distances of the order of a meter. It can be used to compute wavefront statistics over a telescope aperture and is thus directly relevant to AO applications (Voitsekhovich & Cuevas 1995). On the other hand, estimates of the atmospheric phase fluctuations in LBI using $\mathcal{L}_0$ values found here are more model-dependent.

In order to check for vibration effects (wind–shake and guiding), r_0 is computed from absolute image motion in each telescope, corrected for finite $\mathcal{L}_0$ (Borgnino et al. 1992) and compared to r_0 provided by the differential technique. A good agreement is found for ground wind speed up to 15 m/s, showing that telescope vibrations were not significant.

The scintillation index σ_I^2 is computed during data reduction and, as shown by Loos & Hogge (1979), it can give an estimate of the isoplanatic angle when the pupil diameter is around 10 cm. GSM data are also used to derive the effective wavefront speed and its direction (see below) which gives an estimate of the wavefront coherence time. So, this instrument can provide an almost complete set of wavefront parameters relevant to HAR techniques.

3. The GSM campaign at La Silla Observatory

Monitoring of turbulence parameters at La Silla observatory with the GSM was organized in the framework of the ESO VLT Astronomical Site Monitor development program in August-September 1997. At this site the seeing is measured routinely with an automatic ESO DIMM (Sarazin & Roddier 1990) located on a tower 5 m above ground level. The GSM has been installed close to the ESO DIMM. During this campaign GSM data were obtained on 16 nights (a total of 115 hours of $\mathcal{L}_0$, seeing and scintillation measurements). Below we present the first results. Jet stream conditions prevailed during our mission, the seeing being worse (median value 1.7 $''$) and more rapid than average for this season.

3.1. Seeing: comparison with the ESO DIMM

It is interesting to compare the seeing measured simultaneously by the GSM and ESO DIMM. Such comparison is given in Fig. 2 for one night with a moderate ground wind (10 m/s). There is a very good correlation between the seeing variations measured independently by the two instruments. Nevertheless, the

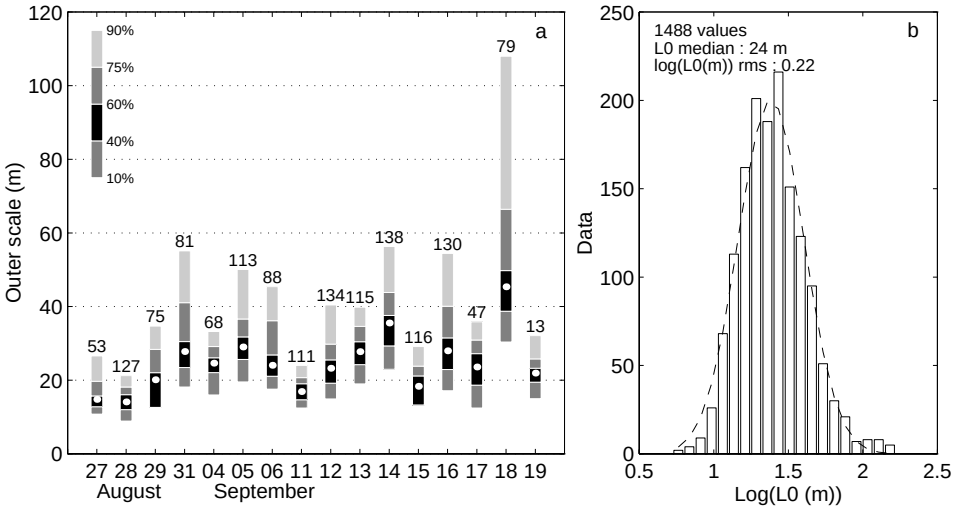

Fig. 4a and b. Summary of the outer scale statistics over 16 nights. **a** For each night the 5 levels of the cumulative distribution of $\mathcal{L}_0$ are shown by grey-scale bars, median values are plotted as circles. Total number of measurements for each night is indicated above the bars. **b** Histogram of $\log\mathcal{L}_0$ for the whole mission with a fitted log-normal distribution (dashed line).

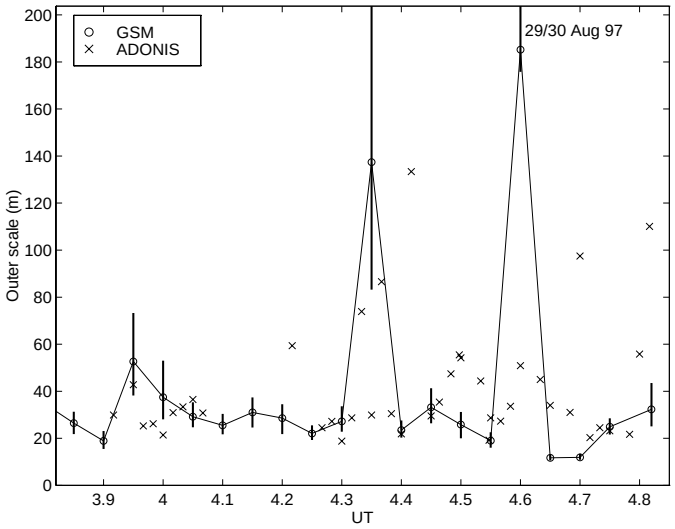

Fig. 5. Comparison of the outer scale values measured simultaneously using GSM and ADONIS. Error bars corresponding to $\pm\sigma$ are shown for GSM data.

GSM measures seeing angles that are systematically greater than those given by the ESO DIMM. This bias can be explained in part by the ground layer turbulence (Fig. 2 after 7h UT), and by the difference between exposure times which are 5 ms and 10 ms for GSM and ESO DIMM, respectively (Fig. 2 before 7h UT). When the GSM exposure time was artificially increased to 10 ms, a good agreement was obtained on nights with strong wind. It means that DIMM data are significantly biased by exposure time effects for strong winds. On another hand a perfect agreement between the GSM and ESO DIMM was found for the periods corresponding to very good seeing (0.6 $''$) and light wind both of which are close to typical conditions at La Silla.

3.2. The wavefront outer scale statistics

Continuous monitoring of the outer scale enables us for the first time to study the temporal variation of $\mathcal{L}_0$ and its correlation with other seeing parameters. As an example, $\mathcal{L}_0$, σ_I^2 and seeing are plotted in Fig. 3 on a logarithmic scale as a function of time for one night. The temporal variation of $\mathcal{L}_0$ shows two characteristic features. Firstly, slow trends with a time scale of hours are noted, just like for the other atmospheric parameters. Secondly, isolated values of large $\mathcal{L}_0$ are observed (arrows in Fig. 3, see also Fig. 5). These "bursts" of $\mathcal{L}_0$ are noted here for the first time. There are no matching rapid variations of seing or scintillation. Thus these bursts correspond only to the transient changes of wavefront spatial structure.

In Fig. 4 the overall statistic of the outer scale is shown. For each night the few characteristic levels of $\mathcal{L}_0$ cumulative distribution and its median are plotted. The night-to-night variability of both median and scatter of $\mathcal{L}_0$ is readily seen. The histogram of $\log\mathcal{L}_0$ for the whole mission is also presented. The $\mathcal{L}_0$ distribution is well approximated by a log-normal one. Its median is 24 m, and rms scatter of $\log\mathcal{L}_0$ is ±0.22, or ±1.67 times. A χ^2 test accepts a log-normal distribution with a significance level of $P(\chi^2) = 0.24$.

On the night of August 29/30 the seeing and wavefront outer scale were simultaneously measured during 1 hour with the ADONIS adaptive optics system (Rigaut et al., 1991; Beuzit et al. 1994) on the ESO 3.6 m telescope. The ADONIS worked in open-loop mode. Outer scale and seeing were calculated from the wavefront tilts recorded by the 7x7 element Shack-Hartmann sensor. A simplified method of $\mathcal{L}_0$ calculation was adopted. The AA variances on the individual wavefront sensor sub-apertures and on the full telescope aperture are computed. Their ratio is used to derive $\mathcal{L}_0$ by the approximate formula given by Ziad et al. (1994). The simultaneous measurements of $\mathcal{L}_0$ with the ADONIS and GSM are plotted in Fig. 5. There is no detailed correlation, which is quite natural because the distance between the GSM and the 3.6 m telescope was more than 1 km. However, the values of $\mathcal{L}_0$ found by both instruments agree well, and the temporal behaviour is also similar, as well as the measured seeing. This comparison proves that GSM data are indeed useful for the analysis and prediction of an AO system performance.

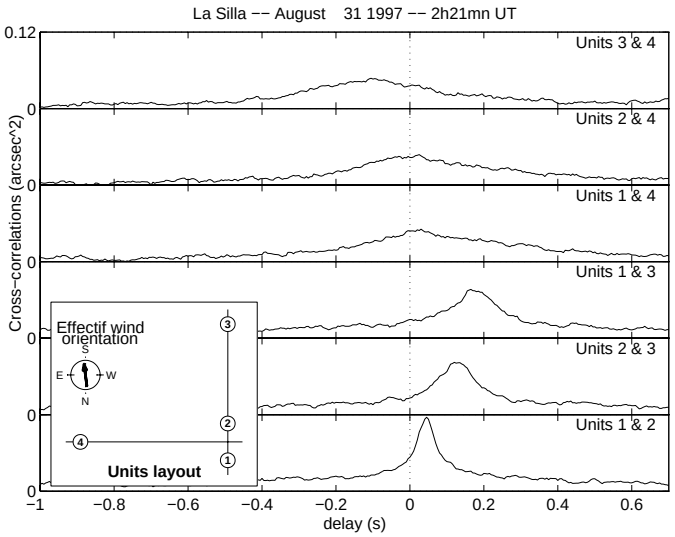

Fig. 6. Temporal cross-correlation functions of the angle of arrival fluctuations at the 6 baselines are plotted on the same scale. The displacement of their maximum is directly related to the projection of the effective wavefront speed on to a given baseline. The instrument configuration and the derived wind speed orientation are shown in the inset. The effective wind speed module is 5.8 m/s.

3.3. Effective wind speed and AO time constant

The temporal evolution of the perturbed wavefront is frequently considered in the framework of the "frozen turbulence" (Taylor) hypothesis, as a constant screen driven by the wind. The analysis of ADONIS data revealed that this situation does indeed occur at La Silla 15% of time (Gendron & Lena 1996). Although the Taylor hypothesis remains a crude approximation of the reality, an effective wavefront speed can be introduced as some average C_n^2-weighted wind speed. Its component along each baseline can be computed either from the phase of the corresponding temporal cross power spectrum of the AA fluctuations (Avila et al. 1997) or, equivalently, as a displacement of the AA cross-correlation function maximum. Here we use the second technique.

The method of effective wind speed measurement with the GSM is illustrated in Fig. 6 where cross-correlation functions of AA are plotted for 6 baselines. From the time lag at each baseline it is found that the wind speed was 5.8 m/s in the NNW direction (ground wind speed was 5.2 m/s from North). In this example, a single dominant layer obeying the Taylor hypothesis provides a good overall description of temporal wavefront evolution. The corresponding AO time constant (Roddier et al. 1982) $\tau = 0.31 r_0/V$ is equal to 4.2 ms at $\lambda = 0.5$ nm.

4. Conclusions

The results of the first systematic monitoring of the wavefront outer scale at La Silla observatory are given. The GSM instrument also produces data on the seeing and effective wavefront velocity. In the near future the isoplanatic angle will be estimated as well, thus providing a complete set of spatial and temporal atmospheric parameters relevant to HAR astronomy. The GSM instrument will be used during the next 2 years for testing several important sites, e.g. Paranal (Chile).

Acknowledgements. The authors would like to thank the La Silla staff for the efficient support of our mission, J.-L. Beuzit for assistance in ADONIS measurements, and all the people of Département d'Astrophysique de l'Université de Nice and of O.C.A. (Observatoire de la Cote d'Azur) who helped us to prepare this measurement campaign. Financial support for this work came from INSU, M.E.N.R.T. and from ESO.

References

Agabi A., Borgnino J., Martin F. et al., 1995, A&AS 109, 557
Avila R., Ziad A., Borgnino J. et al., 1997, J. Opt. Soc. Am. A14, 3070
Beuzit J.-L., Hubin N., Gendron E. et al., 1994, Proc. SPIE 2001, 955
Borgnino J., 1990, Appl. Opt. 29, 1863
Borgnino G., Martin F., Ziad A., 1992, Opt. Comm. 91, 267
Gendron E., Lena P., 1996, ApSS 239, 221
Loos G.C., Hogge C.B., 1979, Appl. Opt. 18, 2654
Martin F., Tokovinin A., Agabi A. et al., 1994, A&AS 108, 1
Rigaut F., Rousset G., Kern P. et al., 1991, A&A 250, 280
Roddier F., Effects of atmospheric turbulence in optical astronomy. In: Wolf E. (ed), Progress in Optics, North Holland, Amsterdam, 1981, p. 281
Roddier F., Gilli J.M., Lund G., 1982, J. Opt. (Paris) 13, 263
Sarazin M., Roddier F., 1990, A&A 227, 294
Voitsekhovich V.V., Cuevas S., 1995, J. Opt. Soc. Am. A12, 2523
Winker D.M., 1991, J. Opt. Soc. Am. A8, 1568
Ziad A., Borgnino J., Martin F,. Agabi A., 1994, A&A 282, 1021